Petrochemistry of Mawgyi andesite and Kanzachaung batholith exposed in Kaba-Magyibin Area, Pinlebu Township

Zaw Win[1], Dr Maung Maung Naing[2] & Dr Min Aung[3]

Abstract

Major- , minor oxides and trace elements of igneous ofKaba-Magyibin area, parts of Wuntho massif, and other analyzed data around the study area are used to discuss the petrochemical characters. According to the chemical classification of various diagram, the andesite of the study area belongs ─ to the basaltic andesite, andesite and dacite clan; within the field of high K-, low K- series; subalkaline and calc-alkaline suit; most of the metaluminous nature. Harker variation diagram of the study area, the granodiorite was suggested that these are derived from the highly evolved melt of magma and fractional crystallization. The granodiorite of the study area shows the calc-alkaline suit of AFM diagram, and peraluminous to metaluminous series, with respect to the mol of [Al_2O_3/ (Na_2O_3+K_2O+ CaO)] and mol of [(Na_2O_3+K_2O)/ Al_2O_3]. Most of the granitoids are typical I-type characteristics. The trace-element data are used in the discrimination of tectonic or geologic provinces associated with particular magma types. The granodiorite and diorite of the study area shows the volcanic-arc granite (VAG), I-type granitoid and upper crust associated with the mantle derived the magmatic arc.

Keywords: Wuntho massif, trace-elements, calc-alkaline, volcanic arc granite (VAG), I-type

[1] Demonstrator, Department of Geology, Mandalay University

[2] Professor, Department of Geology, Yadanabon University

[3] Associated Professor, Department of Geology, Mandalay University

Introduction

The study area, parts of the Wuntho Massif, is situated within the Pinlebu Township, Sagaing Division, and Northern Myanmar. It is bounded by latitude 24° 0' to 24° 15' N and longitude 95° 30' to 95° 45' E within one-inch to one mile scale topographic map 83 P/12 (see Fig.1.1). It covers approximately 240 square miles. Generally, the Pinlebu-Banmauk area lies approximately midway between the south-flowing Ayeyarwaddy River to the east and its major tributary, the Chindwin, to the west, and includes the major mountain range between the two rivers.

Generally, the study area consists chiefly of the various igneous rock types which form a batholith and sedimentary units. The sedimentary units of Kangon formation and Ketpanda formation is the western part, and the eastern part of the research area is mainly composed of igneous units of Kanzachaung batholith such as granodiorite and diorite. The northern flank of the study area found the Mawgyi andesite and sedimentary units.

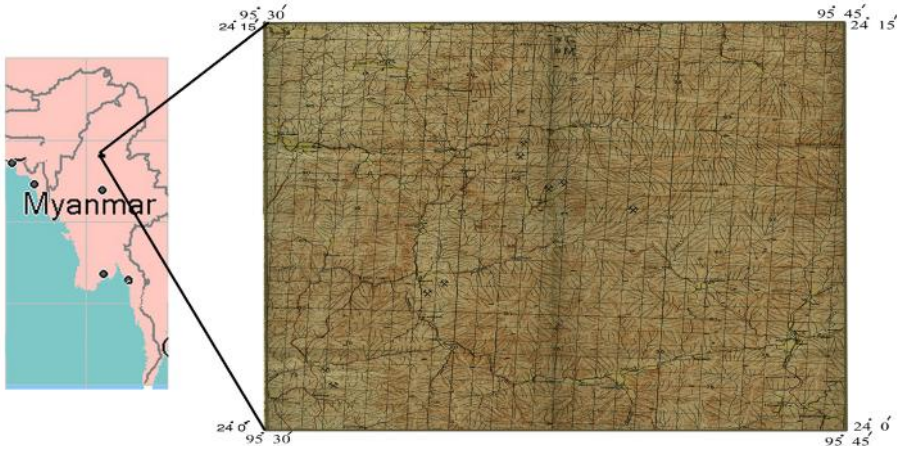

Figure (1) Location map of the study area.

Methods of study

The present study includes field methods and laboratory investigations and employs the three methods to achieve the objectives of the research. The three methods are (a) landsat image and aerial photographic interpretation were made before doing field trip, (b) detailed studies of outcrops and sampling applying the GPS II Plus method and (c) using the XRF analysis to discuss the major and trace element content.

Petrochemistry

Samples were collected from the localities within the study area for the geochemical analysis and were analyzed for both major- and trace element behaviors. The collected samples were prepared and analyzed by the EDXRF at Mandalay University, Physics Department. Nine representative samples of igneous rocks such as andesite, granodiorite and diorite were investigated the major- , minoroxides and trace elements with respect to the standard samples. These nine samples were freshed, lacking any alteration and veining as much as possible. Accuracy and precision for major oxides and trace elements were estimated to be better than 1% relative standard deviation, based on the standard analytical results and precision test. The results of the geochemical analysis of whole-rock major oxides data of andesite, granodiorite and diorite are presented in Table (1), (2) and (3). The result of the trace elements of the andesite, granodiorite and diorite are listed in Table (4).

Table (1) Major oxides composition (in weight %) of the andesite in the study area and it's environ

Rock Type	Mawgyi Andesite					
No.	**1**	**2**	**3**	**1***	**2***	**3***
Sample	ZWMA1	ZWMA2	ZWMA3	YMS2	YMS3	YMS5
Locality	N 24° 10' 20.00" E 95° 34.00' 45.00"	N 24° 14' 50.00" E 95° 36' 30.50"	N 24° 14' 55.00" E 95° 39' 20.50"	83 P/16 and 92 D/4	83 P/16 and 92 D/4	83 P/16 and 92 D/4
SiO_2	57.16	60.1	57.9	52.23	52.86	66.2
TiO_2	0.96	0.7	0.87	0.42	0.50	0.30
Al_2O_3	13.24	16.1	14.3	19.27	12.82	8.28
Fe_2O_3	8.05	6.9	8.79	7.29	8.47	6.58
MnO	0.09	0.15	0.14	0.17	0.18	0.13
MgO	3.9	2.8	3.33	5.59	5.09	2.92
CaO	13.5	5.9	7.79	8.59	13.06	16.41
Na_2O	1.7	3.8	3.48	3.10	5.06	0.27
K_2O	0.28	2.5	2.62	2.51	0.06	0.01
P_2O_5	0.01	0.01	-	0.28	0.28	0.30
Cr_2O_3	0.003	0.003	0.05	-	-	-
LOI	-	-	-	-		
Total	98.89	98.963	99.27	100.25	98.38	101.42

No.1*, 2*, 3* = Data from Ye Min (1992)

Table (2) Major oxides composition (in weight %) of the granodiorite of the study area and it's environ

Rock Type	Granodiorite						
No.	**4**	**5**	**6**	**4***	**5***	**6***	**7***
Sample	ZWGD1	ZWGD2	ZWGD3	YMS6	YMS7	YMS9	YMS10
Locality	N 24°06' 2.22" E 95° 35' 21.3"	N 24° 06' 09.0" E 95° 34' 38.1"	N 24° 07' 39.8" E 95° 38' 49.6"	83 P/16 and 92 D/4	83 P/16 and 92 D/4	83 P/16 and 92 D/4	83 P/16 and 92 D/4
SiO_2	56.8	66.56	69.07	69.68	68.43	60.85	67.15
TiO_2	0.41	0.55	0.48	0.02	0.05	0.20	0.08
Al_2O_3	9.71	14.55	14.75	17.47	17.73	19.96	18.00
Fe_2O_3	3.67	3.26	3.26	0.11	0.30	3.52	0.99
MnO	0.09	0.06	0.07	0.01	0.03	0.14	0.07
MgO	0.76	1.17	0.98	1.24	1.67	1.82	0.96
CaO	21.48	2.79	2.18	1.15	2.87	7.23	3.60
Na_2O	3.67	3.39	3.73	5.58	6.13	4.30	5.68
K_2O	3.13	3.32	4.26	2.57	1.26	2.12	1.76
P_2O_5	0.01	0.13	0.18	0.14	0.14	0.29	0.16
Cr_2O_3	0.01	0.01	0.012	-	-	-	-
LOI	-	-	-	-	-	-	-
Total	99.74	95.79	98.97	97.87	98.61	100.43	98.45

No. 4*, 5*, 6*, 7* = Data from Ye Min (1992

Table (3) Major oxides composition (in weight %) of the diorite exposed in the study area

Rock Type	Diorite		
No.	**7**	**8**	**9**
Sample	ZWD1	ZWD2	ZWD3
Locality	N 24° 09' 04.1" E 95° 37' 29.9"	N 24° 09' 30.5" E 95° 37' 40.30"	N 24° 09' 20.02" E 95° 36' 30.15"
SiO_2	41.19	47.96	30.47
TiO_2	1.15	1.67	1.22
Al_2O_3	10.87	13.6	11.09
Fe_2O_3	10.21	11.72	10.73
MnO	0.24	0.21	0.21
MgO	3.46	3.02	3.59
CaO	26.99	18.03	37.8
Na_2O	4.26	2.04	4.28
K_2O	1.36	1.69	0.41
P_2O_5	0.02	0.014	0.016
Cr_2O_3	0.005	0.009	0.004
LOI	-	-	-
Total	99.755	99.963	99.82

Table (4) Trace elements analysis (ppm) of the Mawgyi andesite, Granodiorite and Diorite

Rock type	Mawgyi andesite			Granodiorite			Diorite		
No.	**1**	**2**	**3**	**4**	**5**	**6**	**7**	**8**	**9**
Sample	ZWMA1	ZWMA2	ZWMA3	ZWGD1	ZWGD2	ZWGD3	ZWGD1	ZWGD2	ZWD3
Locality	N 24° 10' 20.00" E 95°34' 45.00"	N 24° 14' 50.00" E 95° 36' 30.50"	N 24° 14' 55.00" E 95° 39' 20.50"	N 24° 06' 02.22" E 95° 35' 21.30"	N 24° 06' 09.0" E 95° 34' 38.1"	N 24° 07' 39.8" E 95° 38' 49.6"	N 24° 09' 04.1" E 95° 37' 29.9"	N 24° 09' 30.5" E 95° 37' 40.30"	N24°09' 20.02" E95° 36' 30.15"
Rb	5.34	6.17	5.34	88.06	90.44	102.78	38.07	6.99	42.02
Cs	4.0	5.0	4.0	4.0	5.0	6.0	4.0	4.0	4.0
Ba	76.0	78.0	80.2	846.0	810.0	802.0	348.0	110.0	329.0
Sr	87.26	89.02	91.48	261.85	282.33	259.81	454.67	377.25	391.46
Ga	14.9	13.9	15.0	18.8	16.3	17.2	23.9	17.7	23.3
Tl	<1.0	<1.0	<1.0	<1.0	<1.0	<2.0	<1.0	<1.0	<1.0
Ta	<1.2	<1.5	<1.3	<1.2	<1.3	<1.6	<1.2	<1.2	<1.2
Nb	1.4	2.1	3.2	7.9	8.3	9.5	1.4	1.4	4.9
Hf	6.9	7.5	7.0	7.1	8.5	7.5	20.6	19.7	19.9
Zr	69.38	68.60	68.88	132.49	125.27	119.17	79.44	15.72	85.10
Y	26.8	27.3	29.0	20.0	25.0	26.4	20.4	12.1	22.2
Th	<1.0	<1.1	<1.05	10.9	9.5	10.2	5.6	<1.0	3.9
U	<1.0	<1.0	<1.0	<1.0	<1.0	<2.0	<1.0	<1.0	<1.0
La	53.0	57	54.0	71	78	73	68	<2.0	<2.0
Ce	2.0	3.0	2.0	2.0	3.0	6.1	<2.0	<2.0	<2.0
Yb	2.0	2.5	2.1	1.5	3.0	2.2	3.2	1.9	2.4
V	40.5	40.15	44.17	81.76	80.3	72.05	116.67	139.79	213.53
Ni	2.72	3.20	3.5	2.49	3.25	4.24	5.99	3.19	7.0
Cr	23.67	25.36	26.4	98.2	100.2	96.4	39.3	28.3	66.03
Cu	3.48	2.97	3.61	5.22	6.12	5.73	44.59	41.18	50.19
Pb	2.09	2.84	2.98	61.91	62.75	70.28	15.22	5.69	35.39
Zn	19.50	18.58	19.50	124.57	120.65	117.13	110.15	64.17	231.07
Bi	<1.0	<1.0	<2.0	<1.0	<1.5	<1.0	<1.0	<1.0	<1.0
Cd	<2.0	<1.3	<1.5	<2.0	<2.0	<1.0	<2.0	<2.0	<2.0
Sn	<3.8	<2.0	<2.0	<3.8	<3.0	<2.0	<3.8	<3.8	<3.8
W	<3.1	<3.1	<2.0	4.1	5.1	3.7	4.9	3.1	6.4
Mo	<1.0	<1.0	<1.0	<1.0	<1.0	<1.0	<1.0	<1.0	<1.0
Ag	<2.0	<2.0	<2.0	<2.0	<2.0	<2.0	<2.0	<2.0	<2.0
Ge	<0.5	<0.6	<0.5	<0.5	<0.6	<0.5	<0.5	<0.5	<0.5
As	<0.7	<0.4	<0.4	<0.7	<0.4	<0.2	<0.7	<0.7	<0.7
Se	<0.5	<0.8	<0.6	<0.5	<0.5	<2.0	<0.5	<0.5	<0.5
Sb	<4.0	<5.0	<6.0	<4.0	<0.6	<0.4	<4.0	<4.0	<4.0

Petrochemical characters of Mawgyi andesite

According to the chemical classification of Le Bas et al., (1986), based on total alkalis and silica content, the andesite of the study area belongs to the basaltic andesite and andesite clan in Fig.(2). One sample is within the dacite clan. The andesite of the study area falls within the field of Low-K series and High-K series in Fig.(3) following the analysis of Pecerillo and Taylor (1976). Iddings (1892) proposed that all igneous rocks consists the alkaline and subalkaline series. Harker (1909) divided the Cenozoic volcanics bordering the ocean into 'Atlantic' (alkaline) and 'Pacific' (subalkaline) branches. The andesite of the study area plots within the subalkaline series based on the weight percent of SiO_2 and $Na_2O + K_2O$ as shown in Fig. (4) (Mac-Donald, 1968, Irvine and Baragar, 1971). Subalkaline series can be further subdivided into tholeiitic and calc-alkaline type.

The triangular AFM diagram of (Al_2O_3), (FeO_T) and (MgO) of the andesite plots within the field of calc-alkaline, expect one sample which falls in the field of tholeiitic series (Fig.6a). Shand (1927) grouped igneous rocks based on the total molar alkali vs. alumina content as either peralkaline [$Al_2O_3 < (Na_2O+K_2O)$], [$Al_2O_3 > (CaO+Na_2O+K_2O)$], and [$Al_2O_3 < (CaO+Na_2O+K_2O)$]. In the classification of Shand (1927) using the Mol (Al_2O_3 / Na_2O+K_2O+CaO) versus Mol (Na_2O+K_2O / Al_2O_3), the andesite of the study area shows the metaluminous nature (Fig.8). The andesite samples have a wide range in SiO_2 ranging from 52 wt% to 66 wt% and potassium content is high- and low K series. Harker variation diagrams based on the major oxides are drawn using the chemical data obtained by XRF analysis (Fig.5).

Petrochemical characters of granodiorite and diorite rocks

Alfred Harker (1909) proposed that the variation diagram of SiO_2 versus the other major oxides of the rocks show the trend of the continuous magma process, such as magma differentiation or fractional crystallization, assimilation. It can be seen that Al_2O_3, Fe_2O_3 as total iron, TiO_2, CaO, P_2O_5 and MnO decrease with increasing SiO_2. In the K_2O versus SiO_2 diagram, the granodiorite shows high-K characteristics. Variation of Na_2O_3 is not significant (Fig.5). These facts suggest that the granodiorite of the Kanzachaung batholith was derived from the highly evolved melt and fractional crystallization.

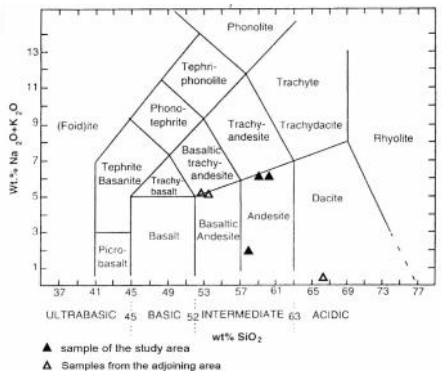

Figure (2) The chemical classification of the Mawgyi andesite based on total alkalis (Na_2O+K_2O) and silica (SiO_2), (Le Bas et al, 1996)

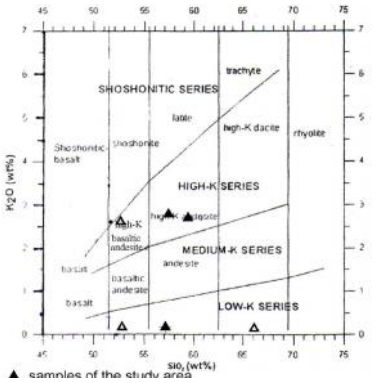

Figure (3) The chemical classification of the Mawgyi andesite based on K_2O – SiO_2 (Peccerillo and Taylar, 1976)

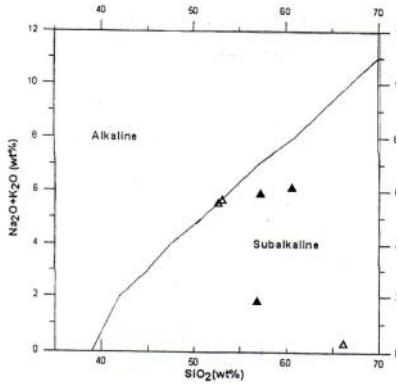

Figure (4) Sub-alkaline nature o the Mawgyi andesite exposed in the area (Mac-Doland, 1996)

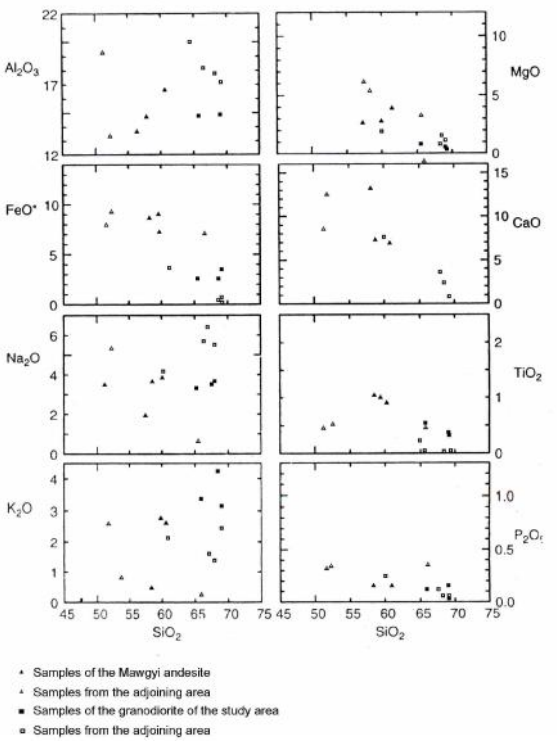

Figure (5) Harker-type variation diagram for the andesite and granodiorite of the study area

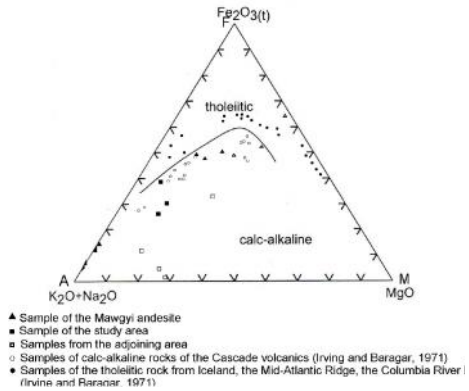

Figure (6) AFM diagram for the granodiorite and Mawgyi andesite of the study area showing the discrimination between tholeiitic

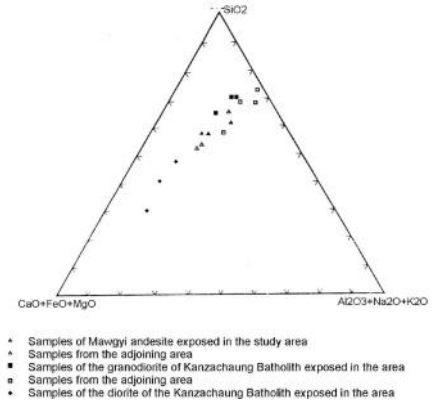

Figure (7) Triangular plot with vertices SiO_2, Al_2O_3+Na_2O_3+K_2O and CaO+MgO+FeO, as used by Steiner (1958)

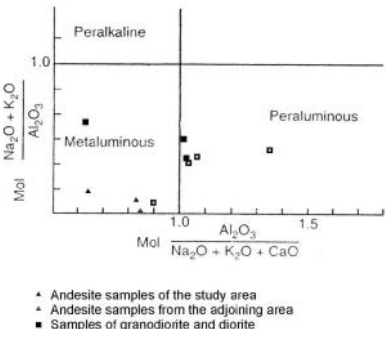

Figure (8) Alumina saturation indices for the andesite, granodiorite and diorite exposed in the area (Shand, 1927)

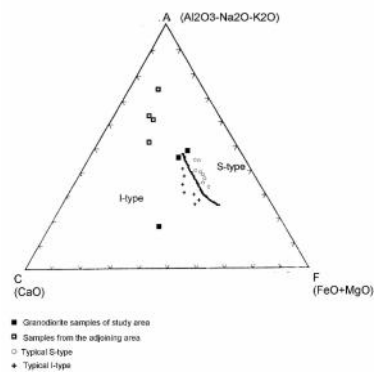

Figure (9) ACF diagram for the granodiorite of the study area compared with the typical I-type and S-type (Hine et al, 1978)

In the AFM diagram of the Al_2O_3, FeO_t and MgO, the granodiorite of the study belongs to the calc-alkaline suite in Fig. (6) (Irvine and Baragar, 1971). Subalkaline series can be further subdivided into tholeiitic and calc-alkaline type. Another triangular diagram (Fig.7) with vertices of SiO_2, Al_2O_3+Na_2O+K_2O and CaO+FeO+MgO is used to display the variation and relation of the andesite, diorite and granodiorite rocks. In this

diagram, alkaluminous oxides (Al_2O_3+Na_2O+K_2O) range is approximately constant variation. These facts suggest that these rocks may be the same parent magma. According to the alumina saturation content of the Shand (1927), the granodiorite of the study area is peraluminous to metaluminous (Fig.8), with respect to the mol of [Al_2O_3 / (Na_2O_3+K_2O+ CaO)] and mol of [(Na_2O_3+K_2O) / Al_2O_3] (Fig.8).

To classify the I-type and S-type granitoid, when plotted on the ACF (Al_2O_3 + Na_2O_3+K_2O, CaO, and FeO+MgO) diagram on the basis of major oxides, it is found that most of the granitoids are of I-type; one plot falls in the S-type field in Fig. (9) (after Hine et at., 1978).

The above mentioned, facts all suggest that the granodiorite of the study area has I-type characteristics on the basis of the schemes of Chappell & White (1974).

Trace element chemistry of the Kanzachaung batholith exposed in the study area

Trace elements of the rocks are more useful to classify the igneous process than the major- and minor oxides because trace elements are far more sensitive to igneous fractionation processes. The trace-element data are used in the discrimination of tectonic or geologic provinces associated with particular magma types. The results of the geochemical analysis of the study area are presented in table (4).

Pearce et al. (1984) classified granite into four main groups: ocean ridge (ORG), volcanic arc (VAG), within plate (WPG), and syncollision granitic rocks (COLG), according to their tectonic environments with the help of trace elements such as Y, Yb, Nb, Ta, and Rb.

The granites within each group may be further subdivided according to their precise settings and petrological characteristics. In the Nb versus Y (Figure 10 a) and Ta versus Yb (Figure 10 b) diagrams, the granodiorite and diorite of the Kanzachaung batholith in the study area plot in the VAG + syn-COLG and VAG fields, respectively. On the Rb- (Y + Nb)(Figure 11 a) and Rb- (Yb + Ta))(Figure 11 b) diagrams, the data of granodiorite and diorite in the study area falls within the volcanic arc granite (VAG).

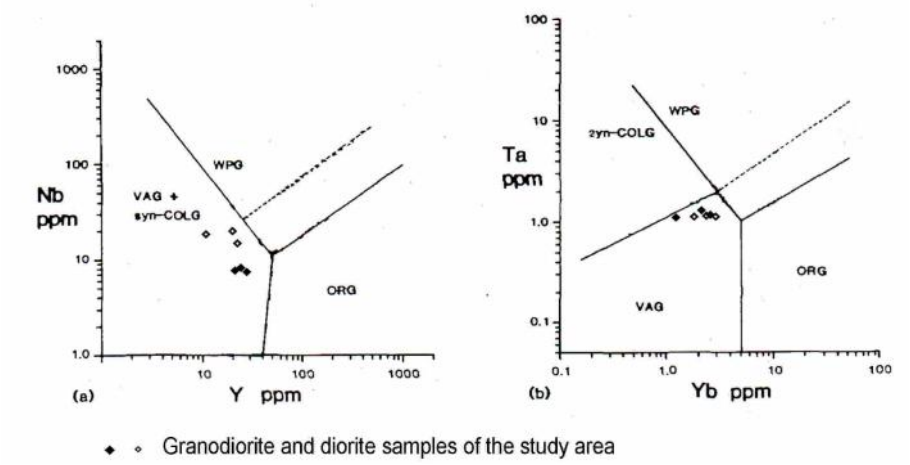

Figure 10) (a) The Nb-Y discrimination diagram for the granodiorite and diorite of the study area showing the field of the volcanic-arc (VAG) and (b) The Yb-Ta discrimination diagram for the granodiorite and diorite of the study area showing the field of the volcanic-arc (VAG) (Pearce et al., 1984)

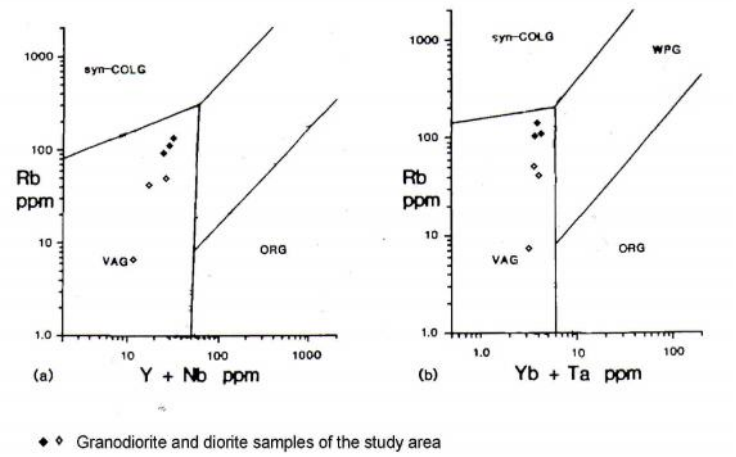

Figure (11) (a) The Rb-(Y+Nb) discrimination diagram for the granodiorite and diorite of the study area showing the field of the volcanic-arc (VAG) and (b) The Rb-(Yb+Ta) discrimination diagram for the granodiorite and diorite of study area showing the field of the volcanic-arc (VAG) (Pearce et al., 1984)

Christiansen and Keith (1996) modified the Pearce's "Trace Element Discrimination Diagrams for the Tectonic Interpretation of Granitic Rocks" by adding the tectonic setting with respect to the I-, S-, M-, A- and OR-type. In the Nb-Y and (Rb-Y+Nb) diagrams, the granodiorite and diorite data cluster in the volcanic-arc (VAG) field with I-type granitoids, except that one sample belongs to the syncollision granite (synCOLG) or S-type (not shown in figure). However, the Rb/Zr versus SiO2 diagram indicates crustal contamination.

In the Hf - Rb/10 - Ta x 3 (Figure 12) and Hf – Rb/30 – Ta x 3 (Figure 13) discrimination diagrams plot the granodiorite and diorite of the study area fall in the volcanic arc granite setting (after Harris et al.,1986).

The Ocean-ridge granite (ORG) – normalized pattern for the granodiorite are characterized by K_2O, Rb and Ba enrichment. However, it is depleted in Zr and Y, indicating the crustal interaction. The comparison of the ORG normalized pattern of the granodiorite with the MORB, the trace element contents of the upper crust and lower crust, the granodiorite of the study area is fairly similar to the upper crust (Figure 14), and LIL elements are enriched with respect to HFS elements.

Generally, the trace elements of Zr (119-133 ppm), Zn (110-120 ppm), and Ga (16-19 ppm) indicate that the granodiorite samples of the study area fall into the field of I-type granitoid.

The average trace element abundance of the granodiorite of the study area is very similar to that of the typical I-type granite, low in large-ion lithophile element (LILE) content, e.g- Rb (88-103 ppm) , Sr (255-283 ppm) and Ba (800-850 ppm) and low in large high field-strength element (HFSE) content, e.g- Nb (7-10 ppm), Zr (119-133ppm), Th (- ppm), U(1 ppm) and Y(20-27 ppm). The transition elements are low to moderate for the granodiorite, e.g- V (70-85ppm), Cr (95-105ppm), Co (3-10 ppm), Ni (2-5 ppm), Cu (5-7 ppm), and Zn (110-120 ppm).

Conclusion

Therefore, the amount of the trace element composition, LILE, HFSE, and normalized value diagram or spider diagram suggest that the granodiorite of the study area is the volcanic-arc granite (VAG), I-type granitoid and upper crust associated with the mantle derived magmatic arc.

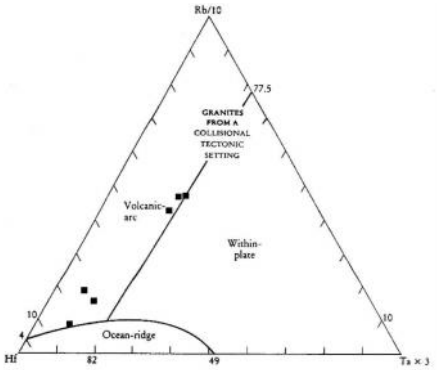

Figure (12) The Hf - Rb/10 – Ta x 3 discrimination diagram for the tectonic setting of the granodiorite and diorite of the study area (Harris et al., 1986)

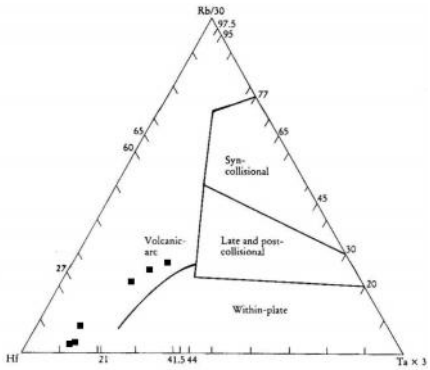

Figure (13) The Hf - Rb/30 – Ta x 3 discrimination diagram for the tectonic setting of the granodiorite and diorite of the study area (Harris et al., 1986)

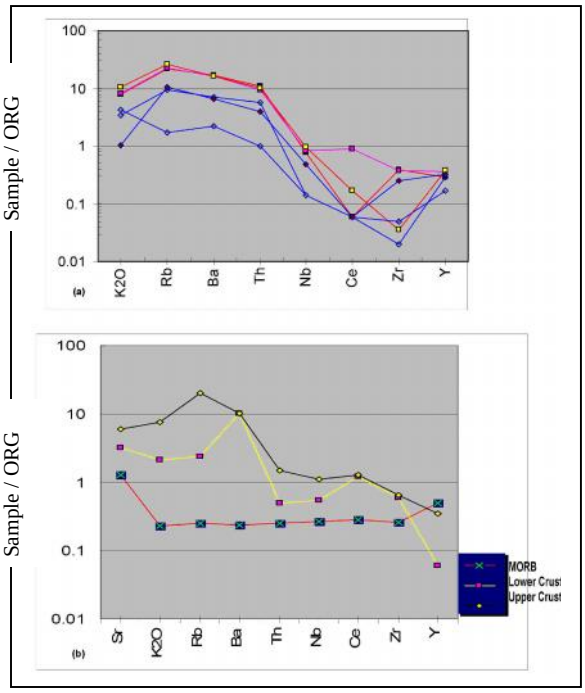

Figure (14) Oceanic ridge granite (ORG) normalized spider diagrams for (a)the granodiorite and diorite of the study area , and (b) MORB, upper crust and lower crust for comparison Normalized value from Pearce et al., (1984)

Acknowledgements

I am deeply indebted to Professor and Head of Department of Geology, Dr Than Than Nu in Mandalay University, for their kind permission and advice to carry out this research work. I wish to express my sincere gratitude to my supervisors, Professor Dr Maung Maung Naing, Department of Geology Yanadabon University and Associated Professor Dr Min Aung, Department of Geology, Mandalay University, for his enthusiastic guidance, valuable criticism and close supervision for research paper.

References

Chappel, B.W., and A.J.R.White, (1992); I- and S-type granites in the Lachlan Fold Belt. Trans. Royal. Sox, Edinburgh, Vol.83,pp 1-26.

Christiansen. E. H., and Keith. J. D., (1996); Trace element systematics in silicic magamas: a metallogenic perspective; in Trace Element Geochemistry of Volcanic Rocks: Applications for Massive Sulfide Explortion, (ed) D. A Wyman; Geological Association of Canada, Notes 12, p.115-151.

Harker, A., (1909); The National History of Igneous Rocks, Macmillan, New York.

Harris N.B., J.A. Pearce, and A.G. Indle, (1986); Geochemical characteristics of collision-zone magmatism, Collision tectonics, Blackwell, Oxford.

Helvaci, C., & M. Satir., 2005; Genetic Relations Between Skarn Mineralization and Petrogenesis of the Evciler Granitoid, Kazdag, Canakkale, Trkey and Comparation with Skarn Granitoids, Journal of Earth Science (Turky), vol. 14, pp. 255-280.

Hine, R., T. S. Williams., B.W Chappell., and A. J. R. White., (1978); Contact between I- and S-typer granitoids of the Koscicusko Batholith, Journal of Geological Society, Austtralia, Vol. 25, pp 219-234.

Irvine T.N., and W.R.A Baragar., (1971); A guide to the chemical classification of the volcanic rocks, Canada Journal of Earth Science, Vol. 8, pp 523-548.

Le Bas M.J., R.W. Lemaitre., A.L. Streckeisen., and B. Zanettin., (1986); A chemical classification of volcanic rocks based on the total alkali-silica diagram, Journal of Petrology, Vol. 27, pp 745-750.

Pearce J.A., B.W. Nigel., Harris., and G. Andrew., and Tindle., (1984) ; Trace Element Discrimination Diagrams for the Tectonic Interpretation of Granitic Rocks, Journal of Petrology, vol. 25, part 4, pp 956-983.

Peccerillo A., and S. R. Taylor.,(1976); Geochemistry of Eocene calc-alkaline volcanics from the Kastamonu area, northern Turkey, Contrib, Mineral, Petrol., Vol. 58, pp 63-81.

Shand S. J., (1927); The Eruptive Rocks, John Wiley, New York.

Steiner, J.S., (1950); Petrogenetic implications of the 1954 Ngauruhoe lava and its xenoliths: N. Z. Jour. of Geol. and Geophy., Vol. 1, pp325-363.

Ye Min, (1992); Geology of the Mingon-Sondaw Area, Wuntho, Banmauk, and Indaw Townships, Mandalay University, (Unpublished).